Loughborough University

This item was submitted to Loughborough's Research Repository by the author.
Items in Figshare are protected by copyright, with all rights reserved, unless otherwise indicated.

# The effect of print speed and material aging on the mechanical properties of a self-healing nanocomposite hydrogel

PLEASE CITE THE PUBLISHED VERSION

https://doi.org/10.1016/j.addma.2020.101253

PUBLISHER

Elsevier BV

VERSION

VoR (Version of Record)

PUBLISHER STATEMENT

This is an Open Access Article. It is published by Elsevier under the Creative Commons Attribution 4.0 Unported Licence (CC BY). Full details of this licence are available at: http://creativecommons.org/licenses/by/4.0/

LICENCE

CC BY 4.0

REPOSITORY RECORD

Sallstrom, Nathalie, Athanasios Goulas, Simon Martin, and Daniel Engstrom. 2020. “The Effect of Print Speed and Material Aging on the Mechanical Properties of a Self-healing Nanocomposite Hydrogel”. Loughborough University. https://hdl.handle.net/2134/12382643.v1.

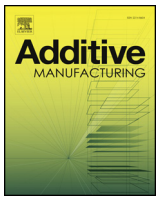
Additive Manufacturing 35 (2020) 101253



Contents lists available at ScienceDirect

Additive Manufacturing

journal homepage: www.elsevier.com/locate/addma



Research Paper

# The effect of print speed and material aging on the mechanical properties of a self-healing nanocomposite hydrogel



Nathalie Sällström[a,*], Athanasios Goulas[a], Simon Martin[b], Daniel S. Engstrøm[a]

[a] Wolfson School of Mechanical Electrical & Manufacturing Engineering, Loughborough University, Loughborough, Leicestershire, LE11 3TU, United Kingdom
[b] Department of Materials, Loughborough University, Loughborough, Leicestershire, LE11 3TU, United Kingdom

ARTICLE INFO

*Keywords:*
Nanoclay-hydrogel
Material extrusion
Printing optimisation
Self-healing
Sulfobetaine methacrylate

ABSTRACT

A UV-curable nanoclay-zwitterionic hydrogel is synthesised and evaluated though rheological and mechanical testing. The results show that aging time of the pre-gel has a big impact on storage and loss of modulus which both increases with increasing aging time, particularly in the first 48 h. The pre-gel is successfully printed and is shown to be able to support itself making it possible to fully print structures before curing. Compression and tensile samples are printed and compared to cast samples. The pre-gel aging time showed that an increased time resulted in a lower strain at failure for both cast and extruded samples. However, when printing with a speed of 10 mm/s with UV-curing during printing, a significant increase in strain at failure is achieved. Furthermore, the compressed samples display self-healing abilities at room temperature and almost completely returns to its original state before compression occurred.

## 1. Introduction

Hydrogels are crosslinked 3D (three-dimensional) polymeric networks which contain a large quantity of water and have been extensively studied for a range of applications such as: tissue engineering [1], drug delivery [2], contact lenses [3], sensors [4], supercapacitors [4] and for wastewater treatment [5]. Additive manufacturing (AM) allows fabrication of complex 3D structures and different AM techniques have been used throughout literature. Extrusion-based 3D printing is the most commonly used technique for hydrogels and is used in this study, but other methods have also been used, including ink-jet techniques [6] laser based techniques (2-photon polymerisation [7] and Stereolithography [6]). Further information about different printing techniques used for hydrogels can be found in literature [8].

Material extrusion techniques has both been used for materials which require support structures and for self-supporting materials. Materials requiring support are commonly printed using suspended layer additive manufacturing (SLAM) where the hydrogel is extruded into a material bath that helps support the material during the printing process [9,10]. Extrusion-based 3D printing without external support is possible when using materials such as nanoclay hydrogels, since the clay inside of the hydrogel works as an internal support, giving the hydrogel its thixotropic and shear thinning properties [11]. Laponite clay consists of discs (1 nm thick and 25 nm in diameter) which are stacked together with a $Na^+$ in between the layers. As Laponite gets dispersed in water, the $Na^+$ dissociate leaving the clay surface with a positive charge. Negative charges also occur around the rims of the platelets due to $OH^-$ dissociation. This charge distribution leads to the platelets forming a 'House of cards' structure which can be disrupted by applying shear forces to the material. The platelets can also rapidly recover back the 'House of cards' structure giving it self-supporting abilities [11] during extrusion printing, which is also known as thixotropic rebuild.

Several studies have been published on extrusion printing of nanoclay-based hydrogels previously for different materials. Zhai et al. developed a nanoclay hydrogel using poly(N-acryloyl glycinamide) (PNAGA) and used a syringe based dispensing technique to print scaffolds for bone regeneration [12]. Jin et al. extruded poly(ethylene glycol) diacrylate (PEGDA)-nanoclay hydrogels with good biocompatibility and low degradation rates [11]. Gao et al. extruded a nanoclay gelatine methacrylate (GelMa) for complex scaffold structures such as a branched vessel and bionic ear [13]. None of the papers on AM of nanoclay hydrogels mention the effect of aging on the printing process or on the mechanical properties of the hydrogels. Although previous studies have explored the effect of aging of Laponite suspensions [14–17], most of them have focused on the rheological properties and non on the potential effect it might have on mechanical properties. This work will look into this as well as the effect of other printing parameters.

* Corresponding author.
*E-mail address:* S.M.N.Sallstrom@lboro.ac.uk (N. Sällström).

https://doi.org/10.1016/j.addma.2020.101253
Received 6 February 2020; Received in revised form 13 March 2020; Accepted 13 April 2020
Available online 11 May 2020
2214-8604/ © 2020 The Author(s). Published by Elsevier B.V. This is an open access article under the CC BY license (http://creativecommons.org/licenses/BY/4.0/).

In this contribution, a zwitterionic sulfobetaine methacrylate monomer (N-(3-Sulfopropyl)-N-methacroyloxyethyl- *N,N*-dimethylammonium betaine (SPE)) was used within a nanoclay hydrogel system for developing a soft, potentially non-fouling material for biomedical applications. A zwitterionic monomer was chosen due to its potential to be non-fouling at the same time as not being cytotoxic [18]. These non-fouling properties are believed to be caused by the balanced charge of the zwitterions which may prevent protein absorption on the surface. Non-fouling properties are useful as it provides a way of controlling cell growth by using a combination of cell adhesive and non-fouling materials [19] which is important for general tissue engineering applications. The application in mind during the development of this material is soft prosthetic sockets for fully integrated next generation prosthetics which have a connection to the users own nervous system. Current prosthetic sockets are commonly made from a hard-polymeric material which does not adapt to dimensional changes of the residual limb. This will lead to poorly fitting sockets which are very uncomfortable to the user. The aim of the hydrogel material developed in this work is therefore to be soft with an ability to recover from compressive forces to adapt to dimensional changes of the residual limb. Herein, rheological and mechanical characterisations (both compression and tensile) will be used to evaluate the effect of varying hydrogel composition, printing parameters and pre-hydrogel aging times for both cast and printed samples. The ability of the material to recover from compressive forces will also be investigated.

## 2. Experimental section

### 2.1. Hydrogel fabrication

Laponite XLG (BYK Additives) was dispersed in degassed deionised (DI) water using magnetic stirring for 20 min. N-(3-Sulfopropyl)-N-methacroyloxyethyl- *N,N*-dimethylammonium betaine (SPE) (Merck Chemicals, UK) were then mixed in the dispersed Laponite at a varying wt.% of monomer and Laponite. Once fully dispersed, 0.4 wt.% Irgracure 2959 (Sigma-Aldrich, UK) was added.

For cast samples, this material was directly poured into moulds and was either UV-cured directly or stored at 90 % humidity (to prevent drying) and cured after 48 h. UV-curing occurred at 365 nm for 1 h at an intensity of 2.2 mW/cm$^2$.

The material used for printing was loaded into 5 mL syringes (Beckton Dickinson, New Jersey, United States), wrapped in aluminium foil and stored in a dark environment from 5 h up to 12days.

### 2.2. Rheology

Rheological properties of the pre-gel suspensions (before UV-cured) were measured using an Anton Paar Physica MCR 101 high shear rheometer with a parallel-plate geometry (25 mm in diameter and a gap distance of 0.7 mm). To determine the storage modulus (G') and loss modulus (G)", a continuous ramp test was conducted with varying shear rate from 0.01 to 100s$^{-1}$ and an amplitude sweep mode was used for all of the testing. The rheological properties of different composition as well as different aging times (for the 10 wt% SPE 6 wt% Laponite composition) was evaluated.

### 2.3. 3D printing

All manufacturing experiments were carried out on a multi-process additive manufacturing kit (System 30 M, Hyrel3D, Norcross, GA, USA), equipped with a dispensing module (SDS-5, Hyrel3D, Norcross, GA, USA), using 5 mL luer-lock syringes (Becton Dickinson, Franklin Lakes, New Jersey, USA) and 250 μm needles of 0.5 in. in length (Adhesive Dispensing, Milton Keynes, United Kingdom). The SDS-5 module was fitted with an array of λ = 365 nm UV-LEDs (Fig. 1). The material used for printing experiments was a hydrogel comprising of 10 wt.% SPE and 6 wt.% Laponite. Prior to printing the material was left inside an enclosed syringe barrel to settle for 5 h except for the aging studies. A range of different speeds (5–20 mm/s) were used, to evaluate the effect of printing speeds on the mechanical properties of the resultant 3D printed structures. A constant positive displacement value of 90 pulses per microlitre was applied throughout all printing runs.

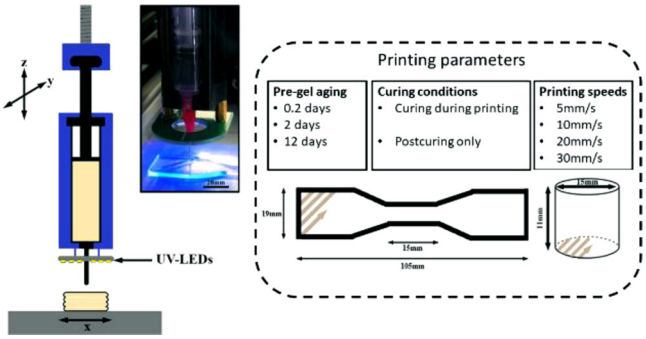



**Fig. 1.** Diagram and picture of the 3D suspension system and the printing parameters evaluated. The platform moved in x direction while the syringe dispenser moved in y and z direction. Samples were printed at 45° rastering angle with 100 % infill density.

### 2.4. Mechanical characterisation

All of the mechanical testing was performed on as-prepared hydrogels and 5 samples were tested for each variable. Variables included; different printing speeds, different aging of the pre-hydrogel material, varying the post-curing time and using curing during printing or only post-curing.

#### 2.4.1. Tension

Cast and 3D printed tensile samples, prepared according to the ASTM D638-14 type IV standard (with 50 % length reduction) were tested using a universal testing machine (Instron 5944, High Wycombe, Buckinghamshire, United Kingdom) fitted with a 2 kN load cell. All tests were performed at a speed of 10 mm/s until sample failure. Stress and strain values were automatically calculated using the kit's proprietary software (Bluehill 3, Instron, High Wycombe, Buckinghamshire, United Kingdom). Screw side tensile grips were used to hold the hydrogel in place during testing.

#### 2.4.2. Compression

Cast and printed compression samples with a diameter of 15 mm and a height of 11 mm were tested in a universal testing machine (H50KS, Tinius Olsen, Salfords, United Kingdom) fitted with a 1 kN load cell and compression plates. A speed of 0.1 mm/s was used for all compression tests. The hysteresis testing had an idle time of 2 min between each cycle and a total of 10 loading and unloading cycles was performed for each sample. Each cycle compressed the sample up to a distance of 80 % of its initial height and not until failure as samples would not fail before the safety limit of the testing machine was reached.

## 3. Result and discussion

### 3.1. Rheology

Rheological evaluations were performed to see the effect of the hydrogel's composition as well as aging time on the rheological properties. The full data graphs of the effect of both composition and aging time can be seen in Fig. 2. As seen in the graphs, the crossover point for G' and G" (yield point ($\tau_0$)) occurs at lower and lower shear rates for increased aging time and at an increased modulus. $\tau_0$ indicates a

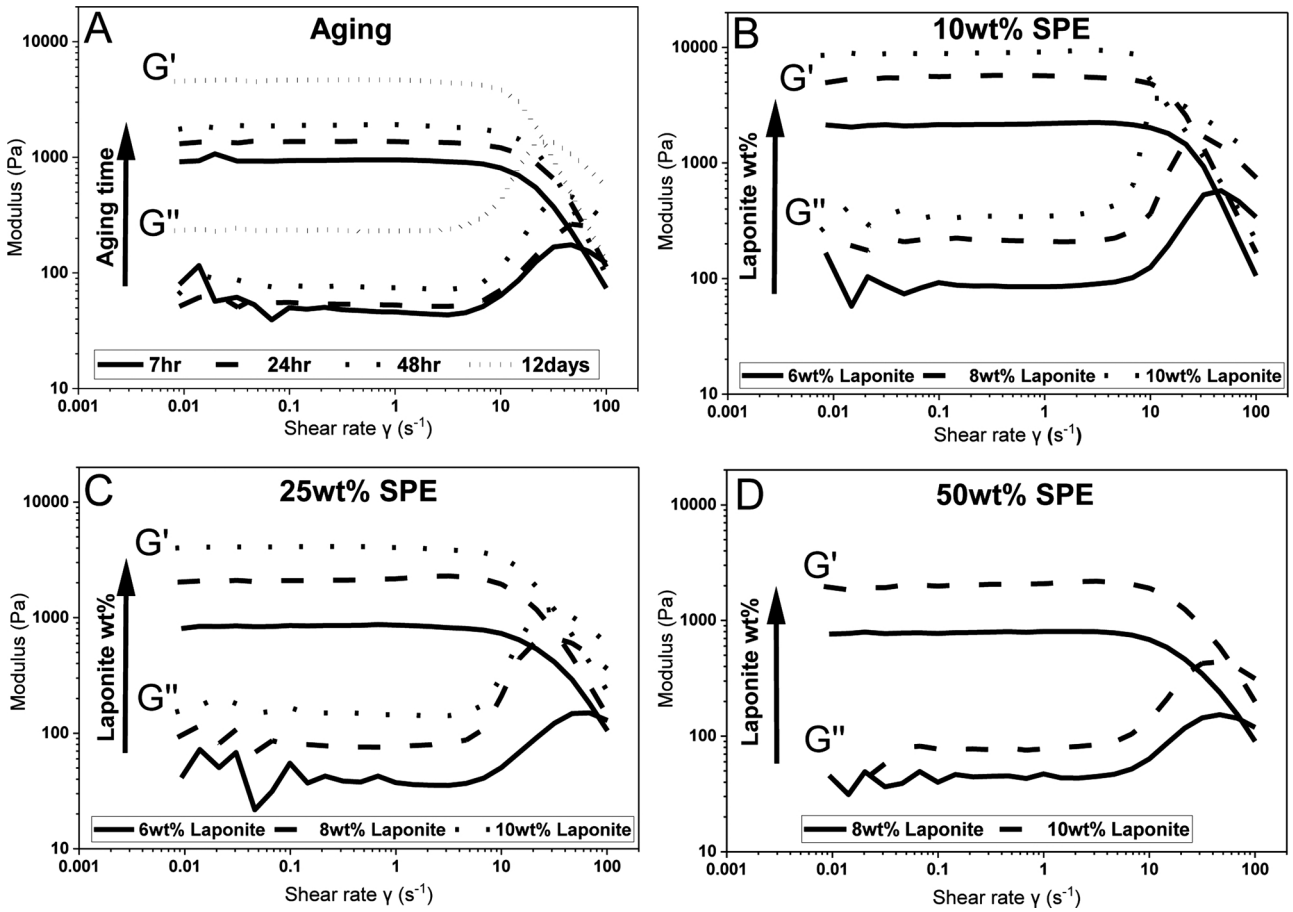



**Fig. 2.** The effect of aging time (A) and composition (B, C, & D) on storage (G') and loss (G") modulus. G' is the top lines while G" is the bottom lines. For complete data set, see Figure S1, supporting information.

transition of the material from a solid-like state to a liquid-like state [16,20]. Moreover, increased clay content was also showed to move $\tau_0$ towards a lower shear rate and increase in monomer content showed the reverse effect with increase in shear rate (for complete data, Table S1 and Table S2, supporting information). To successfully 3D print a material through extrusion, the material needs to be shear thinning, G' should be above G" for low shear rates (this means that the material has enough storage modulus to retain its own weight) and finally have a fast thixotropic rebuild time. This study shows that the developed material has shear thinning properties as well as having G' over G" for lower shear rates and thus should be able to support itself during printing. Previous thixotropic research on nanoclay hydrogels has shown to give a very rapid re-build time of 0.08 s which occurs due to rapid recovery of its house of cards structure [11]. The material developed in this work should have similar recovery due to the same nano-clay system being used. This means that the printing time between layers could be as low as 0.08 s as the material can support its own weight after that time which helps give an indication of possible printing speeds.

The effect of Laponite and monomer content as well as aging time at a shear rate of $1s^{-1}$ (where G' and G" appeared stable for all conditions) can be seen in Fig. 3. Increased Laponite content results in increased G' and G" whereas for the increased monomer content the reverse effect is observed. This means that at some loadings, e.g. 10 wt.% SPE 6 wt.% Laponite, 25 wt.% SPE 8 wt.% Laponite and 50 wt.% SPE 10 wt.% Laponite, the modulus is very similar. An increase in both G' and G" means that there is an increase in both viscous and elastic properties of the material. This means that for the increased Laponite content, a higher force would be needed to extrude the material while an increase in monomer requires reduced forces. Increased aging time showed an increase in both G' and G" as well, which may be caused by structural rearrangement occurring over time to reach a lower energy state. Laponite-water suspensions are known to continuously undergo rearrangement which increases the viscosity as well as the elasticity [16] which would explain the result obtained herein. The suspensions with an aging time below 7 h will not be printable through extrusion due to too low modulus, the same can be said for some of the compositions (50 wt% SPE 8 wt% Laponite & 25 % SPE 6 wt% Laponite). On the other hand, some suspensions would be too viscous after preparation to load the material into syringes without causing bubbles (10 wt% SPE 10 wt % Laponite). The other compositions should be printable by altering printing parameters (such as speed and pressure). Furthermore, it is also important to consider the desired mechanical properties of the hydrogel when deciding on the composition to use and not only consider the rheological properties. Herein, the 10 wt% SPE and 6 wt% Laponite composition was used for the printing and mechanical testing.

### 3.2. 3D printing

The pre-hydrogel material was easy to print and did not require significant parameter optimisation to print successfully. The material could also support itself well (since G' > G"), meaning a printing-then-curing approach could be used. Even after aging the material for 12 days prior to printing, the material was still successfully printed, however, upon curing the material turned increasingly opaque (Fig. 4D), compared to the low-age time material (Fig. 4C). This could be an indication of phase separation occurring within the hydrogel upon curing. Scaffolds with low infill density could successfully be

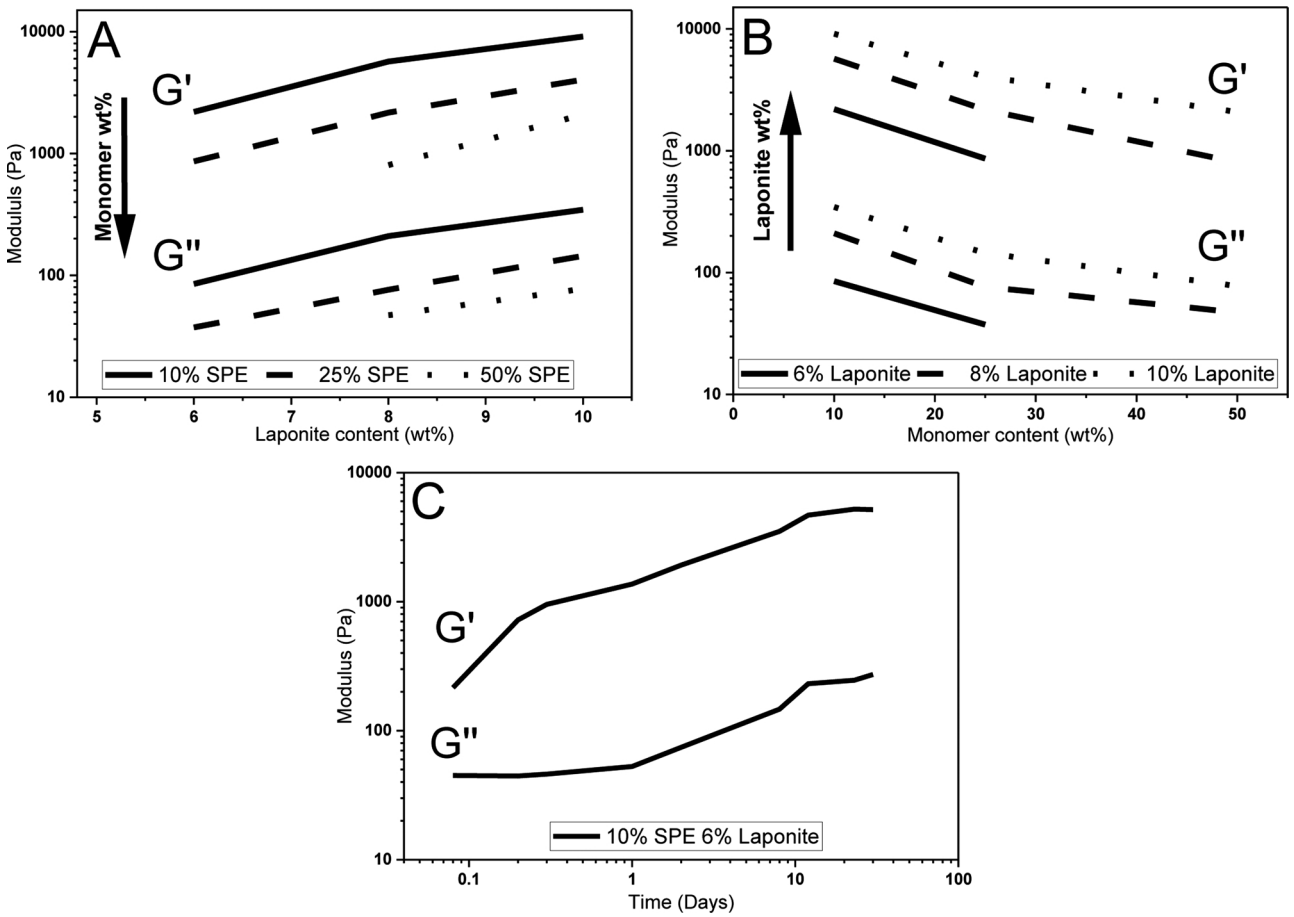



**Fig. 3.** G' and G" data at a shear rate ($\gamma$) of $1s^{-1}$ for A - varying Laponite content B- varying monomer content and C - varying aging times.

printed without curing or support structures and did not collapse (Fig. 4F). Compression as well as tensile samples were printed and mechanically tested and compared to cast samples which are explained in following sections.

### 3.3. Mechanical characterisation

#### 3.3.1. Tensile testing

Tensile testing of samples made using different printing parameters, curing and aging times were compared to tensile testing performed on

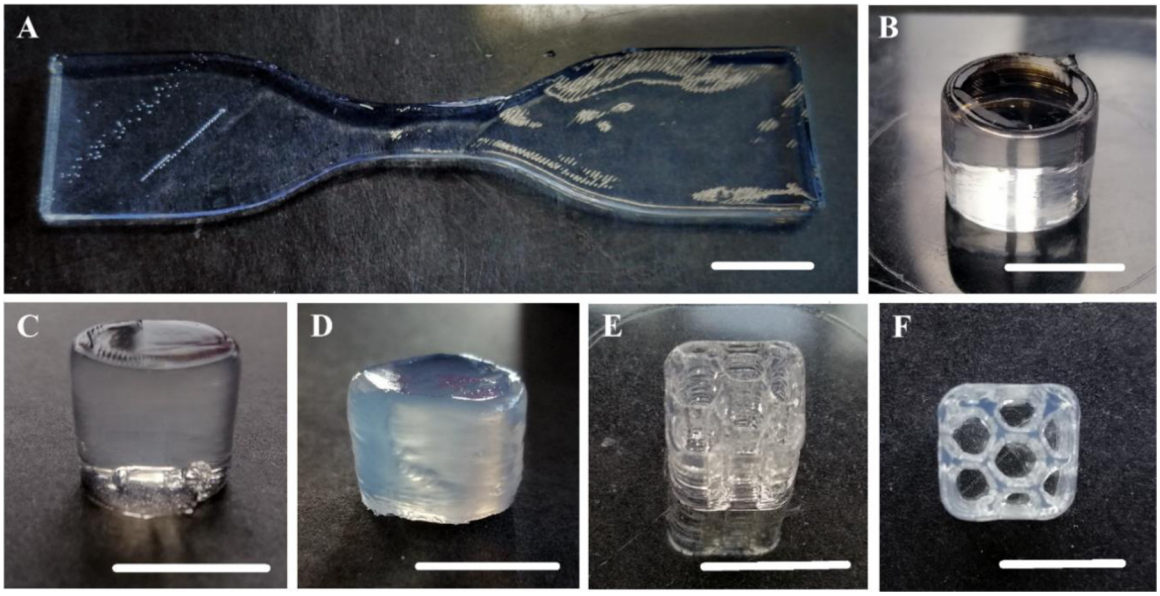



**Fig. 4.** Different printed parts, each scale bar represents 10 mm. A- tensile sample B- compression sample before curing. C- same compression sample after curing, D- compression sample with 12 days aged material after curing E- Scaffold structure printed without curing with 10 % infill density F – top view of the same scaffold which demonstrates the self-supporting ability of the material.

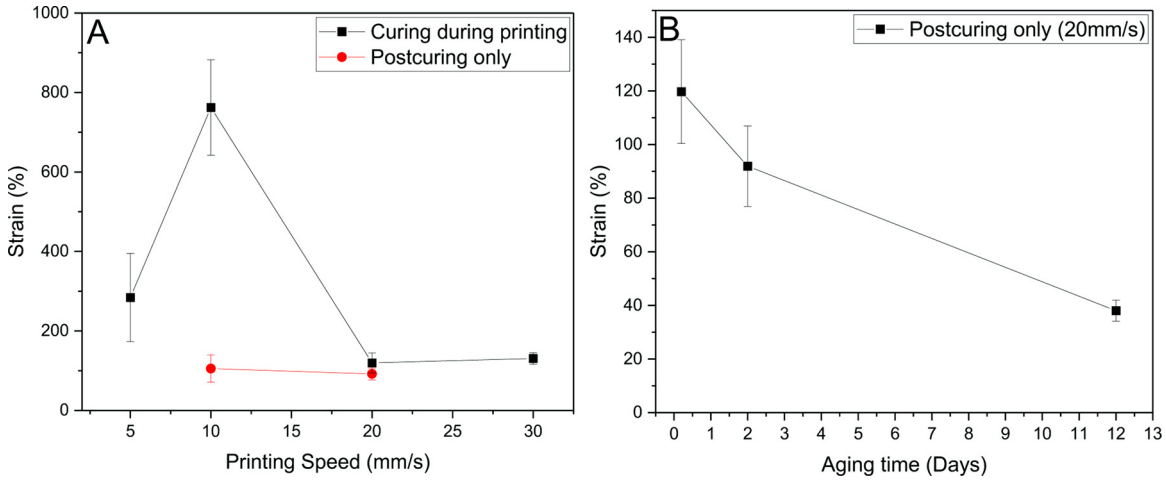



**Fig. 5.** Graphs showing the effect of A- printing speed and curing during or after printing and B- aging time on tensile strain at failure. No clear trends on the effect of printing speed or aging on UTS, stress at failure and Young's modulus was observed, see Table S3, supporting information. For complete stress and strain graphs see Figure S4-S7, supporting information.

cast samples. The result showed that the printing speed had a big impact on tensile properties if the samples are cured during printing, however, if the samples are only post-cured then the speed did not appear to have any noticeable effect (Fig. 5A). A printing speed of 10 mm/s significantly increased the strain at failure, even higher than for that of the cast samples (898.3 ± 248.8 % for the non-aged cast samples and 239.7 ± 51.2 % for the 48 h aged cast samples, see Table S3, supporting information). It is worth noting that the printing speed also affected the curing time, since a slower print resulted in increased exposure to the UV-light. Therefore, experiments were also conducted to evaluate the effect of curing time on mechanical properties, this data can be found in Fig. S2, supporting information. The result showed that even reduced UV-intensity (50 %) for the 10 mm/s printing speed still showed improved mechanical properties compared to the 20 mm/s printing speed and thus the speed itself is having an impact on failure strain (Fig. S3, supporting information).

There is a large difference in viscosity from the directly prepared and aged material, which could potentially affect the polymerisation process. It is well known that viscosity does have an effect on polymerisation. Lower viscosity permits greater monomer mobility which helps in propagating the free-radical polymerisation process [21]. With increased viscosity, as seen with aged pre-hydrogel suspension, it is therefore possible that shorter polymer chains (lower molecular weight) are obtained and this affects the mechanical properties. Previous research has shown that higher molecular weight is required to achieve greater tensile strains in nanoclay hydrogels [22] which is also observed herein. It was hypothesised that increasing the shear applied during printing by increasing the speed would reduce the viscosity enough to achieve a better polymerisation, however, this was shown not to be the case. Lower printing speed displayed improved elongation at break which is potentially a consequence of the material having more time to rebuild the molecular structure between layer deposition. Alternatively, this effect may depend on the molecular weight of the hydrogel. The later scenario is supported by the fact that the printing speed had no effect on strain at failure when curing does not occur during printing. The sample printed at 5 mm/s did not show improved strain from the 10 mm/s printed sample, this could be because of the bottom layer being cured for much longer than the top layer which also caused warping of the edges to occur. The shear force caused by the printing is important for the curing process, but it seems like a lower shear force increases the strain at failure. This could potentially be caused by having less disruption of the clay's 'house of cards' structure which may also influence the mechanical properties. However, this cannot be confirmed from this study.

Furthermore, increased aging time of the pre-gel material (before printing/curing), also showed to have a negative impact on tensile properties, particularly the strain at failure (Fig. 5B). Previous studies have evaluated the effect of aging of water-Laponite suspensions. Laponite particles in water-suspensions are considered to be trapped by the neighbouring particles. The trapped particles can then undergo structural re-arrangements to reach a lower energy state. In Laponite suspensions, this low-energy state occurs when there are strong laponite particle interactions which does not get disrupted even with high shear [16]. This irreversible particle aggregation is also called overlapping coin configuration [15] or collapsed house of cards structure [23]. The house of cards structure formation is considered reversible and the particles can remain dispersed. This has been previously confirmed to be the case through electron microscopy techniques. It is possible that the suspension aged at 12 days could have reached its irreversible coin configuration and thus even with the shear applied during printing, the clay-structure cannot successfully be disrupted enough to work as a cross-linker within the system, leading to the significant decrease in strain at failure.

### 3.3.2. *Compression testing*

The data obtained from compression testing displays less dependence on different printing parameters used (Fig. 6). There is no significant difference between different printing speeds (Fig. 6A), but the aging does seem to have some effect on the compression properties (Fig. 6B). The non-aged cast samples reach significantly less compression stresses than the 48 h aged samples at the same strain. However, not much difference is seen between the 48 h aged samples and the 12 days aged samples (Fig 6C). The elastic modulus does increase with increasing age time meaning that aging does increase the stiffness of the hydrogel (Table S4, supporting information). Previous studies on PEG materials have shown that Young's modulus does indeed increase for decreased molecular weights [24]. This result may therefore further confirm that the increase viscosity for the aged samples may have an effect on the polymerisation process, creating lower molecular weight hydrogels. However, other studies have shown that there is no effect of molecular weight on Young's modulus for high density polyethylene [25] and some have even shown increased Young's modulus with increased molecular weight (PVDF nanofibers) [26]. This is very likely to be dependent on the polymer and manufacturing method as well and not only the molecular weight.

It is important to consider the material stiffness for biomedical applications as stiffness can alter cellular behaviours. For example, research has showed that mesenchymal stem cells can respond on surface

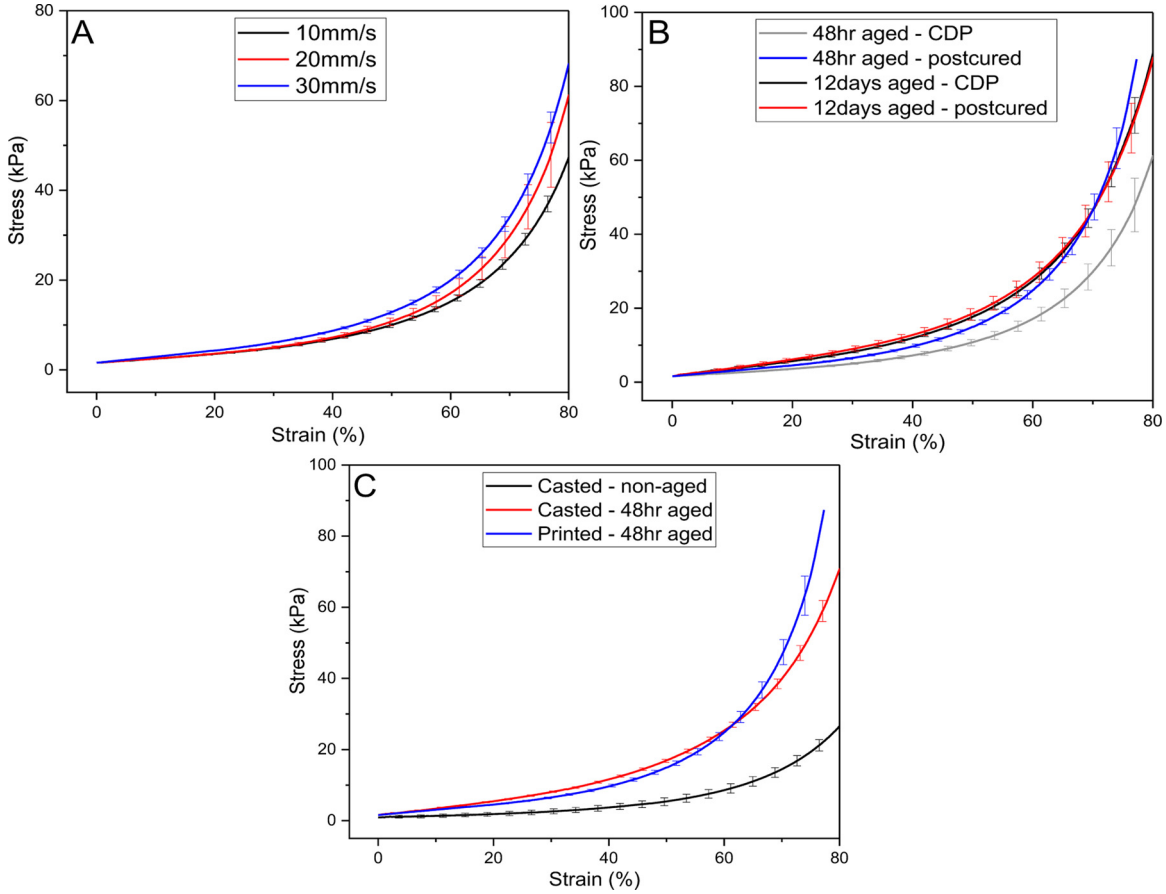



**Fig. 6.** Compression graphs of averaged data with standard deviation error bars for different printing parameters and aging times. A – Data for different printing speeds, all printing speeds used curing during printing (CDP). B – Different aging time data with or without CDP. C – Cast samples (aged or non-aged) compared to printed sample (printed at 20 mm/s without curing during printing).

stiffness where soft materials (0.1–1 kPa) results in neuron formation and stiffer materials (8–17 kPa) led to myoblast formation or osteoblast formation (25–40 kPa) [27]. Some studies has also shown that increased stiffness of hydrogels causes decreased cellular adhesion of 3T3 Fibroblasts [28]. Low material stiffness has also shown to create longer neurites than stiffer materials [29,30]. The low stiffness seen of the hydrogels in this study (~0.1–1.3 kPa for Young's modulus and ~0.1 − 0.3 kPa for compression modulus) may therefore be advantageous for neural applications. Furthermore, softer hydrogels have also shown to reduce adhesion of gram-positive and gram-negative bacteria [31]. Moreover, work conducted in the lab using a neuroblastoma cell line showed no cytotoxic responses of the hydrogel and extended neurites were observed, further demonstrating the hydrogels suitability for neural applications [32].

Images of the compression samples was taken before, directly after and after certain time points to evaluate the recovery of the hydrogel (Fig. 7) As seen in the images, the hydrogel almost recovers back to its original state, apart from a dent seen in the centre of the gel. Self-healing hydrogels have previously been reported in literature to be dependent on the reversibility of the crosslinks used. Different kinds of bonding have successfully shown self-healing mechanisms, reviews of this has previously been published [33,34]. Other zwitterionic nanoclay crosslinked hydrogels shown to be self-healing is said to be caused by diffusing grafted polymer chains that interacts with nearby clay particles through hydrogen bonding which forms new crosslinks and can thus fuse separated surfaces together. This can only occur above the UCST (Upper critical solution temperature), below this healing cannot occur due to formation of ion pairs [35]. This means that the hydrogel developed in this work can self-heal at room temperature and would also be able to do so at body temperature which could be a very useful property to have for tissue-engineering applications.

*3.3.2.1. Compression hysteresis*. Compression hysteresis tests showed that the printing speed has no significant effect on hysteresis recovery, however, increased aging time does reduce the recovery between the cycles (Fig. 8B). This is very likely to be affected by the molecular weight as mentioned previously. Previously reported research has shown that a reduced molecular weight reduces the ductility of materials [36] which suggests what is happening in this case. The area seen between the loading and unloading curve is the dissipated energy. As seen in Fig. 8A, the first loading and unloading curve displays the greatest dissipated energy which gets reduced for the following cycles. This shows that the material has good ability to dissipate energy and rapid recovery of properties of the hydrogel which commonly means that the material is highly elastic and have high toughness. This is usually seen in materials containing nanoclay crosslinkers and is believed to be as a consequence of the bonding between the clay particles and the polymer chains being physical bonds. This allows deformed polymer chains to detach from the clay to partially release the elastic energy stored in the material [11,37]. Furthermore, printing speed does seem to have a small effect on the dissipated energy with increased speeds and increased age time as well causing increased energy dissipation (Fig. 8B). This could be caused by the detachment of an increased number of chains from the clay which may have something to do with the possibly lower molecular weight for the aged samples.

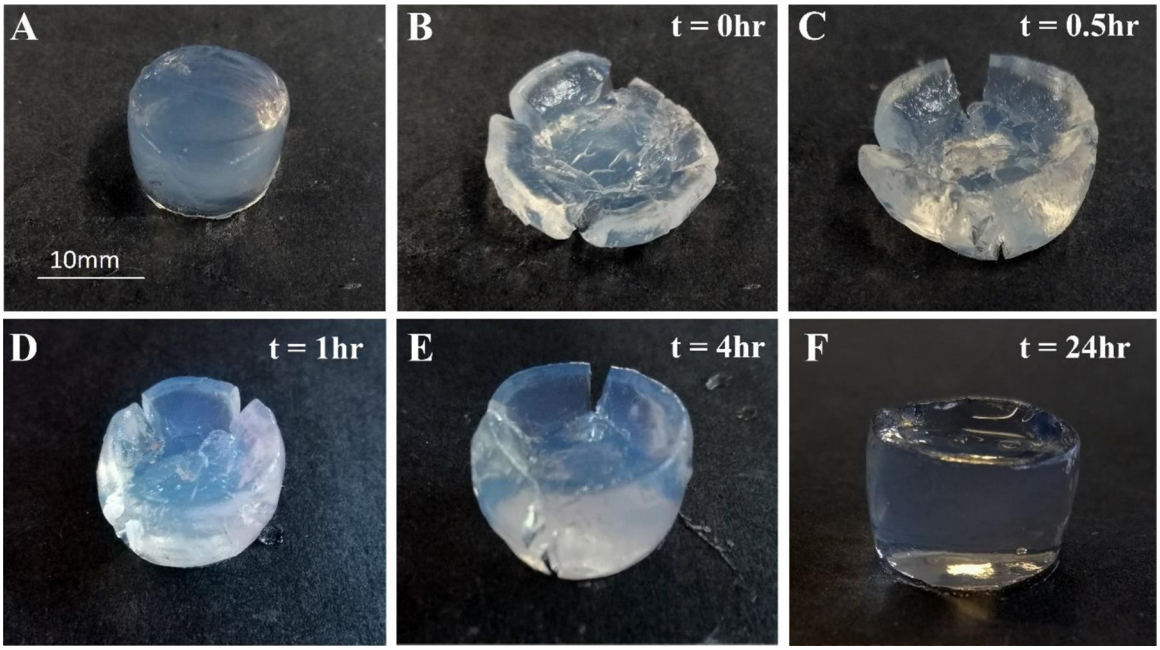



**Fig. 7.** Images of the recovery after compression for the 12days aged samples, at room temperature in an enclosed environment to prevent water evaporation. A - before compression, B - 1 min after compression, C - 30 min after compression D −1 h after compression.

## 4. Conclusion

In this work a nanoclay-crosslinked zwitterionic sulfobetaine hydrogel was successfully 3D printed with both curing during printing and a printing-then-curing approach. The effect of monomer and Laponite content as well as aging time of the pre-hydrogel on rheological properties was evaluated. Increased monomer content resulted in reduced G' and G'' while Laponite showed the reverse effect. Increased aging time also showed an increase in G' and G'' which may have something to do with the structure reaching a lower energy state and adapting an overlapping coin formation. Aging as well as printing speeds did have a significant effect on the tensile properties, particularly the strain at break. Compression tests did not show much of a dependence on printing parameters, however, for compression hysteresis test aging does seem to have an effect on the ability of the material to recover as well as the dissipated energy. It was shown that it is important to use curing during printing to improve mechanical properties which may indicate that the reduced viscosity during printing have an effect on the free-radical polymerisation and potentially achieves higher molecular weight hydrogels. The hydrogel also showed self-healing abilities and recovered well from compression at room temperature. This work shows promising properties of the material to be used in printing of tissue engineering scaffolds. Cell culture studies conducted in previous work also support this.

## Data availability

The raw data required to reproduce these findings are available to download from: https://doi.org/10.17028/rd.lboro.11793948.

## CRediT authorship contribution statement

**Nathalie Sällström:** Conceptualization, Methodology, Investigation, Visualization, Writing - original draft. **Athanasios Goulas:** Investigation, Writing - review & editing. **Simon Martin:** Conceptualization, Supervision, Writing - review & editing. **Daniel S. Engstrøm:** Conceptualization, Supervision, Writing - review & editing.

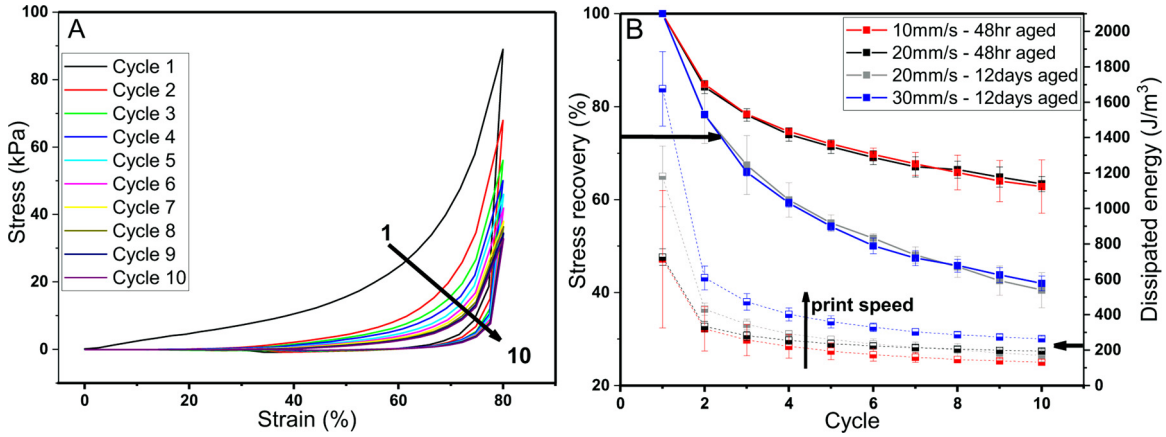



**Fig. 8.** A - Example of hysteresis curve for one of the printed samples (10 mm/s – 12days aged) with data from all cycles. B - Curve showing the stress recovery (solid lines) between the different cycles as well as the dissipated energy (dashed lines with hollow boxes) for different printing speeds as well as aging times (Dissipated energy calculated as the area between loading and unloading curve).

## Declaration of Competing Interest

The authors declare that there are no conflicts of interest.

## Acknowledgement

EPSRC Centre for Doctoral Training in Additive ManufacturingEP/L01534X/1.

## Appendix A. Supplementary data

Supplementary material related to this article can be found, in the online version, at doi:https://doi.org/10.1016/j.addma.2020.101253.

## References

[1] K. Yue, G. Trujillo-de Santiago, M.M. Alvarez, A. Tamayol, N. Annabi, A. Khademhosseini, Synthesis, properties, and biomedical applications of gelatin methacryloyl (GelMA) hydrogels, Biomaterials 73 (2015) 254–271.
[2] T.R. Hoare, D.S. Kohane, Hydrogels in drug delivery: progress and challenges, Polym. (Guildf) [Internet] 49 (8) (2008) 1993–2007, https://doi.org/10.1016/j.polymer.2008.01.027 Available from:.
[3] A. Mühlebach, B. Müller, C. Pharisa, M. Hofmann, B. Seiferling, D. Guerry, New water-soluble photo crosslinkable polymers based on modified poly(vinyl alcohol), J. Polym. Sci. Part A Polym. Chem. 35 (16) (1997) 3603–3611.
[4] A. Baldi, M. Lei, Y. Gu, R.A. Siegel, B. Ziaie, A microstructured silicon membrane with entrapped hydrogels for environmentally sensitive fluid gating, Sens. Actuators B Chem. 114 (1) (2006) 9–18.
[5] R.M. Shamsuddin, C.J.R. Verbeek, M.C. Lay, Settling of bentonite particles in gelatin solutions for stickwater treatment, Procedia Eng. [Internet] 148 (2016) 194–200, https://doi.org/10.1016/j.proeng.2016.06.570 Available from:.
[6] V.A. Liu, S.N. Bhatia, Three-dimensional photopatterning of hydrogels containing living cells, Biomed. Microdev. 4 (4) (2002) 257–266.
[7] A.A. Pawar, G. Saada, I. Cooperstein, L. Larush, J.A. Jackman, S.R. Tabaei, et al., High-performance 3D printing of hydrogels by water-dispersible photoinitiator nanoparticles, Sci. Adv. 2 (4) (2016) 1–8.
[8] T. Billiet, M. Vandenhaute, J. Schelfhout, S. Van Vlierberghe, P. Dubruel, A review of trends and limitations in hydrogel-rapid prototyping for tissue engineering, Biomaterials [Internet] 33 (26) (2012) 6020–6041, https://doi.org/10.1016/j.biomaterials.2012.04.050 Available from:.
[9] J.J. Senior, M.E. Cooke, L.M. Grover, A.M. Smith, Fabrication of complex hydrogel structures using suspended layer additive manufacturing (SLAM), Adv. Funct. Mater. 1904845 (2019) 1904845.
[10] Y. Jin, W. Chai, Y. Huang, Printability study of hydrogel solution extrusion in nanoclay yield-stress bath during printing-then-gelation biofabrication, Mater. Sci. Eng. C [Internet] 80 (November) (2017) 313–325, https://doi.org/10.1016/j.msec.2017.05.144 Available from:.
[11] Y. Jin, C. Liu, W. Chai, A. Compaan, Y. Huang, Self-supporting nanoclay as internal scaffold material for direct printing of Soft hydrogel composite structures in air, ACS Appl. Mater. Interfaces [Internet] 9 (May (20)) (2017) 17456–17465, https://doi.org/10.1021/acsami.7b03613 Available from:.
[12] X. Zhai, Y. Ma, C. Hou, F. Gao, Y. Zhang, C. Ruan, et al., 3D-printed high strength bioactive supramolecular polymer/clay nanocomposite hydrogel scaffold for bone regeneration, ACS Biomater. Sci. Eng. 3 (6) (2017) 1109–1118.
[13] Q. Gao, X. Niu, L. Shao, L. Zhou, Z. Lin, A. Sun, et al., 3D printing of complex GelMA-based scaffolds with nanoclay, Biofabrication [Internet] 11 (April (3)) (2019) 035006. Available from: http://stacks.iop.org/1758-5090/11/i=3/a=035006?key=crossref.ce1b4b8cf732f0423dd740690941fb8f.
[14] A. Shahin, Y.M. Joshi, Hyper-aging dynamics of nano-clay suspension, Langmuir 28 (13) (2012) 1–29.
[15] A. Shahin, Y.M. Joshi, Physicochemical effects in aging aqueous laponite suspensions, Langmuir [Internet] 28 (November (44)) (2012) 15674–15686, https://doi.org/10.1021/la302544y Available from:.
[16] A. Shahin, Y.M. Joshi, Irreversible aging dynamics and generic phase behavior of aqueous suspensions of laponite, Langmuir 26 (6) (2010) 4219–4225.
[17] R.K. Pujala, H.B. Bohidar, Ergodicity breaking and aging dynamics in Laponite-Montmorillonite mixed clay dispersions, Soft Matter 8 (22) (2012) 6120–6127.
[18] K.-T. Huang, Y.-L. Fang, P.-S. Hsieh, C.-C. Li, N.-T. Dai, K.-T. Huang, Zwitterionic nanocomposite hydrogels as effective wound dressings, J. Mater. Chem. B [Internet] 4 (23) (2016) 4206–4215. Available from: http://xlink.rsc.org/?DOI=C6TB00302H.
[19] L. Chen, C. Yan, Z. Zheng, Functional polymer surfaces for controlling cell behaviors, Mater. Today [Internet] 21 (January (1)) (2018) 38–59, https://doi.org/10.1016/j.mattod.2017.07.002 Available from:.
[20] A. M'Barki, L. Bocquet, A. Stevenson, Linking rheology and printability for dense and strong ceramics by direct ink writing, Sci. Rep. 7 (1) (2017) 1–10.
[21] B.W. Brookz, Viscosity effects in the free-radical polymerization of methyl methacrylate, Proc. R. Soc. Lond. A Math. Phys. Eng. Sci. [Internet] 357 (1689) (1977) 183–192. Available from: www.jstor.org/stable/79443.
[22] H. Takeno, Y. Kimura, Molecularweight effects on tensile properties of blend hydrogels composed of clay and polymers, Polymer (Guildf) [Internet] 85 (2016) 47–54, https://doi.org/10.1016/j.polymer.2016.01.008 Available from:.
[23] T. Abraham, N. Lam, J. Xu, D. Zhang, H. Wadhawan, H.J. Kim, et al., Collapse of house-of-cards clay structures and corresponding tailings dewatering induced by alternating electric fields, Dry Technol. [Internet] 37 (9) (2019) 1053–1067, https://doi.org/10.1080/07373937.2018.1482313 Available from:.
[24] Z. Chen, D. Zhao, B. Liu, G. Nian, X. Li, J. Yin, et al., 3D Printing of Multifunctional Hydrogels, Adv. Funct. Mater. 29 (20) (2019) 1–8.
[25] W.G. Perkins, N.J. Capiati, R.S. Porter, The effect of molecular weight on the physical and mechanical properties of ultra-drawn high density polyethylene, Polym. Eng. Sci. 16 (3) (1976) 200–203.
[26] B. Zaarour, L. Zhu, X. Jin, Controlling the surface structure, mechanical properties, crystallinity, and piezoelectric properties of electrospun PVDF nanofibers by maneuvering molecular weight, Soft Mater [Internet] 17 (2) (2019) 181–189, https://doi.org/10.1080/1539445X.2019.1582542 Available from:.
[27] G.N. Li, D. Hoffman-Kim, Tissue-engineered platforms of axon guidance, Tissue Eng. Part B Rev. 14 (1) (2008) 33–51.
[28] A.M. Jonker, S.A. Bode, A.H. Kusters, J.C.M. Van Hest, D.W.P.M. Löwik, Soft PEG-hydrogels with independently tunable stiffness and RGDS-content for cell adhesion studies, Macromol. Biosci. 15 (10) (2015) 1338–1347.
[29] R.K. Willits, S.L. Skornia, Effect of collagen gel stiffness on neurite extension, J. Biomater. Sci. Polym. Ed. 15 (12) (2004) 1521–1531.
[30] X. Cao, M.S. Shoichet, Photoimmobilization of biomolecules within a 3-dimensional hydrogel matrix, J. Biomater. Sci. Polym. Ed. [Internet] 13 (6) (2002) 623–636, https://doi.org/10.1163/156856202320269120#.VwyH2PkrLIU Available from:.
[31] K.W. Kolewe, S.R. Peyton, J.D. Schiffman, Fewer bacteria adhere to softer hydrogels, ACS Appl. Mater. Interfaces 7 (35) (2015) 19562–19569.
[32] N. Sällström, A. Capel, M.P. Lewis, D. Engstrom, S. Martin, 3D-printable Zwitterionic Nano-composite Hydrogel System for Biomedical Applications, (2020).
[33] D.L. Taylor, In het panhuis M. Self-healing hydrogels, Adv. Mater. 28 (41) (2016) 9060–9093.
[34] Q. Li, C. Liu, J. Wen, Y. Wu, Y. Shan, J. Liao, The design, mechanism and biomedical application of self-healing hydrogels, Chin. Chem. Lett. [Internet] 28 (9) (2017) 1857–1874, https://doi.org/10.1016/j.cclet.2017.05.007 Available from:.
[35] K. Haraguchi, J. Ning, G. Li, Changes in the properties and self-healing behaviors of zwitterionic nanocomposite gels across their UCST transition, Macromol. Symp. 358 (1) (2015) 182–193.
[36] L.M. Nicholson, K.S. Whitley, T.S. Gates, J.A. Hinkley, Influence of molecular weight on the mechanical performance of a thermoplastic glassy polyimide, J. Mater. Sci. 35 (24) (2000) 6111–6121.
[37] H. Jiang, G. Zhang, X. Feng, H. Liu, F. Li, M. Wang, et al., Room-temperature self-healing tough nanocomposite hydrogel crosslinked by zirconium hydroxide nanoparticles, Compos. Sci. Technol. [Internet] 140 (2017) 54–62, https://doi.org/10.1016/j.compscitech.2016.12.027 Available from:.